THE EUROPEAN
PHYSICAL JOURNAL C

CrossMark

Search for single production of vector-like top partner decaying to *Wb* at *eγ* collision

Bingfang Yang[2], **Hongbo Shao**[3], **Jinzhong Han**[1,a]

[1] School of Physics and Telecommunications Engineering, Zhoukou Normal University, Henan 466001, China
[2] College of Physics and Materials Science, Henan Normal University, Xinxiang 453007, China
[3] College of Science, Hebei Agricultural University, Baoding 071000, China

Abstract In a simplified model including an $SU(2)$ singlet T quark with charge 2/3, we investigate the single vector-like T production at the high energy $e\gamma$ collision. We study the observability of the vector-like T focusing on the $T \rightarrow Wb$ decay channel with $W \rightarrow l\bar{\nu}$ at $\sqrt{s} = 2.0$ TeV. In this analysis, only two free parameters are involved, namely the T quark coupling strength for single production g^* and the mass m_T. We scan the parameter space and find that the correlation region of $g^* \in [0.24, 0.5]$ and $m_T \in [800, 1360]$ GeV can be excluded with integrated luminosity $L = 100\,\text{fb}^{-1}$ and the correlation region of $g^* \in [0.13, 0.5]$ and $m_T \in [800, 1620]$ GeV can be excluded with integrated luminosity $L = 1000\,\text{fb}^{-1}$ at 2σ level.

1 Introduction

A number of theories beyond the Standard Model (SM) offer mechanisms to resove the quadratic divergences that arise from the radiative corrections to the Higgs boson mass so as to solve the naturalness problem [1]. One solution is to introduce vector-like quarks (VLQs) [2,3], defined as hypothetical spin-1/2 coloured particles whose left- and right-handed components have the same transformation properties under the SM gauge group. VLQs could dampen the unnaturally large quadratic corrections to the Higgs boson mass by contributing significantly to loop corrections. They appear in many scenarios, such as extra dimensions [4,5], little Higgs [6–10] and composite Higgs models [11,12]. In this analysis, we focus on a simplified model including the $SU(2)$ singlet vector-like top quark (T).

Recently, the direct searches for the vector-like T at 13 TeV LHC have been performed by ATLAS [13] and CMS [14] Collaborations relying on signatures induced by

both the vector-like T pair-production and single-production modes, corresponding to an integrated luminosity of about 36 fb^{-1}. Assuming 100% branching ratio to Wb, the observed (expected) 95% CL lower limits on the T mass are 1350 GeV (1310 GeV). Assuming 100% branching ratio to Zt, the observed (expected) 95% CL lower limits on the T mass are 1160 GeV (1170 GeV).

Compared to the complicated QCD background at the LHC, the lepton colliders can offer much cleaner experimental environment. Some design schemes have been put forward, such as the International Linear Collider (ILC) [15,16] and the Compact Linear Collider (CLIC) [17,18], they can run at the center of mass (c.m.) energy ranging from 500 GeV to 3 TeV. Along with e^+e^- collision, other options such as $\gamma\gamma$ and $e\gamma$ collider modes [19–23] can also be realized by the backward Compton scattering of incident electron- and laser-beams. Each option for colliders will provide interesting topics to study, here we will focus on the search for the single vector-like T production at $e\gamma$ collision, which will allow unique opportunity to investigate the vector-like top quark.

The paper is organized as follows. In Sect. 2 we give a brief description of the simplified model including the vector-like T with charge 2/3. In Sect. 3 we investigate the signal and discovery potentiality of the vector-like T in the Wb channel at the $e\gamma$ collision. Finally, we draw our conclusions in Sect. 4.

2 Top partner in a simplified model

Recently, a generic parametrization of an effective Lagrangian for top partners has been proposed in [24], where the vector-like quarks are embedded in different representations of the weak $SU(2)$ group. Here, we focus on the simplified case that the heavy vector-like T quark of charge 2/3 is an $SU(2)$ singlet, with couplings only to the third generation of SM

[a] e-mail: hanjinzhong@zknu.edu.cn

Springer
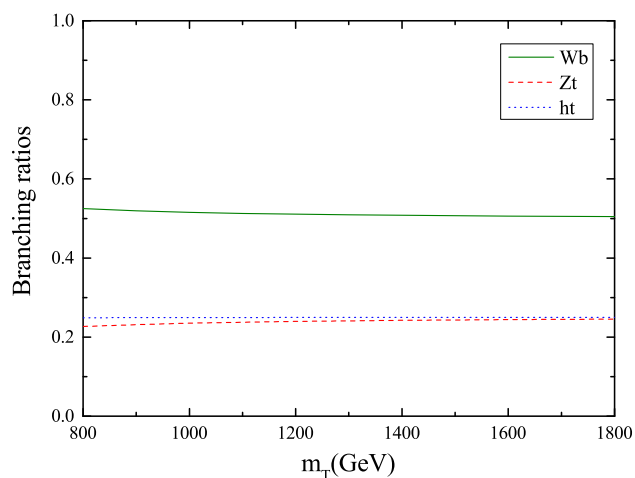
Fig. 1 Branching ratios of the top partner decay

quarks. The results based on this simplified effective theory can be used to make predictions for more complex models including various types of top partners. The general effective Lagrangian of the top partner sector can be described by

$$\mathcal{L}_T = \frac{g g^*}{2\sqrt{2}} \left[\bar{T}_L W_\mu^+ \gamma^\mu b_L + \frac{g}{\sqrt{2} c_W} \bar{T}_L Z_\mu \gamma^\mu t_L \right.$$
$$\left. - \frac{m_T}{\sqrt{2} m_W} \bar{T}_R h t_L - \frac{m_t}{\sqrt{2} m_W} \bar{T}_L h t_R \right] + h.c., \quad (1)$$

where m_T is the top partner mass and g^* parametrizes the single production coupling associated with the SM quarks.

g is the $SU(2)_L$ gauge coupling constant, $c_W = \cos\theta_W$ and θ_W is the Weinberg angle. In this simplified model, there are only two free parameters, i. e. the top partner mass m_T and the coupling parameter g^*.

Generally, the top partner couplings to the SM particles are severely constrained by electroweak precision physics as well as by the direct measurement of V_{tb} [25]. However, such constraints can be altered significantly in most realistic models including the vector-like quark with two or more partner multiplets [26–33]. Here we take a conservative limit for the coupling parameter $g^* \leq 0.5$, which is consistent with the current experiment bounds [34].

The vector-like T quark has three possible decay modes: $T \to ht$, $T \to Zt$ and $T \to Wb$, and their branching ratios are shown in Fig. 1. For $m_T > 800$ GeV, the branching ratios $Br(T \to ht) \approx Br(T \to Zt) \approx \frac{1}{2} Br(T \to Wb)$ is a good approximation as expected by the Goldstone boson equivalence theorem [35].

## 3 Event generation and discovery potentiality

In Fig. 2, we show the leading order Feynman diagram of the process $e^- \gamma \to \nu_e b \bar{T}$.

We extract the model file [36] of the singlet vector-like top partner by using the package **FeynRules** [37]. Then, we use **MadGraph 5** [38] to calculate the leading order cross sections of the process $e^- \gamma \to \nu_e b \bar{T}$. We scan over the free
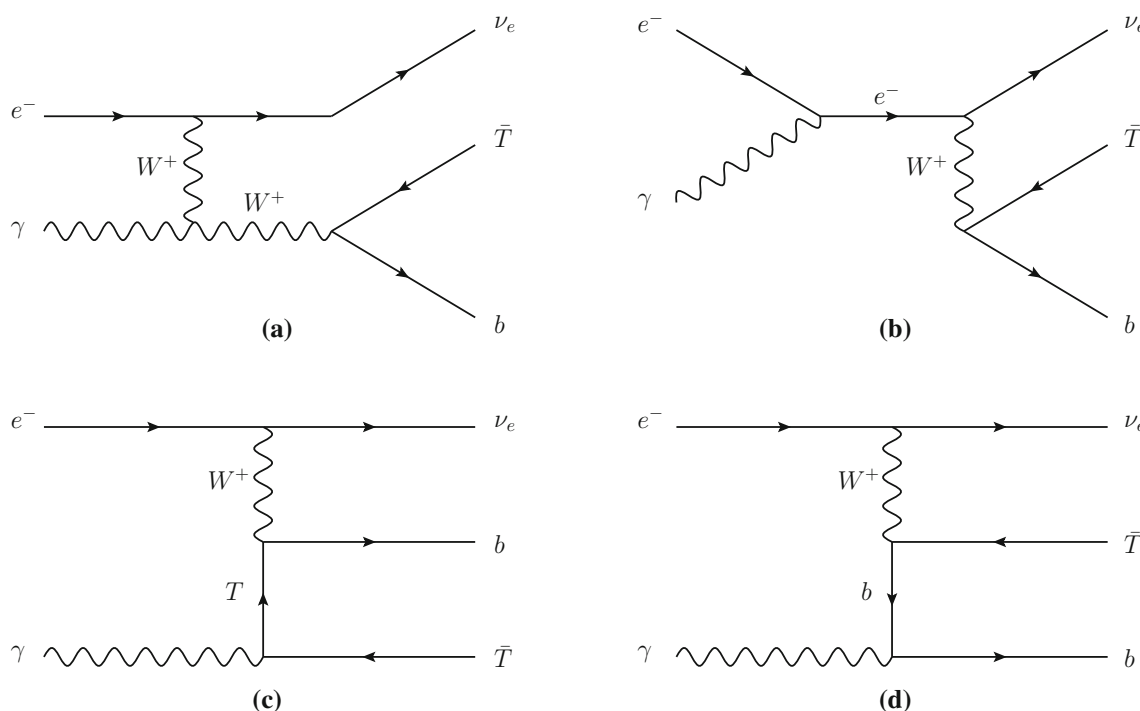
Fig. 2 Leading order Feynman diagram of the process $e^- \gamma \to \nu_e b \bar{T}$
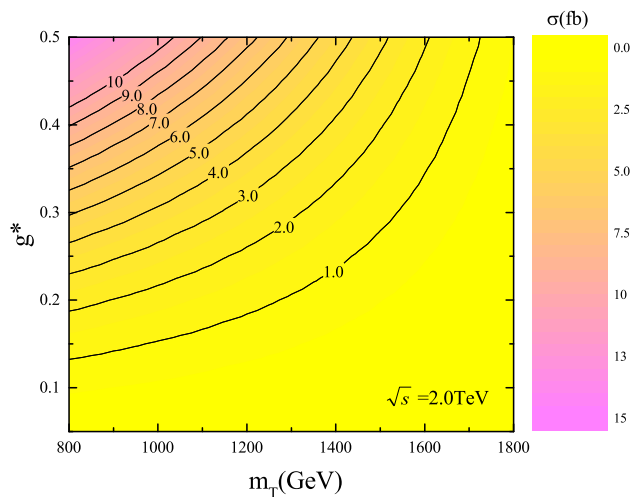
Fig. 3 The cross sections of the top partner on the $g^* \sim m_T$ plane at $\sqrt{s} = 2.0$ TeV

parameters m_T and g^* within the region $m_T \in [800, 1800]$ GeV and $g^* \in [0.0, 0.5]$, and take the SM parameters as follows [39]

$$\sin^2 \theta_W = 0.231, \ \alpha_e = 1/128, \ M_Z = 91.1876 \text{GeV},$$
$$m_t = 173.5 \text{GeV}, \ m_h = 125 \text{GeV}.$$

In Fig. 3, we show the cross sections σ on the $g^* \sim m_T$ plane at the c.m. energy $\sqrt{s} = 2.0$ TeV. We can see that the cross sections decreases with the increase of the top partner mass m_T and increases with the increase of the coupling parameter g^*. In the favorable parameter space, the cross sections can reach more than 10 fb.

In next section, we will perform the Monte Carlo simulation and explore the discovery potentiality of top partner T through the channel

$$e^- \gamma \to \nu_e b \bar{T} \to \nu_e b W^- (\to l^- \bar{\nu}_l) \bar{b} \to l^- + 2b + \not{E}_T, \quad (2)$$

which implies that the events contain one isolated charged lepton $l^- (l = e, \mu)$, two b-jets and missing transverse energy $\not{E}_T$.

For this signal, the most relevant backgrounds come from $\nu_e b \bar{t}$, $\nu_e W Z$ and $\nu_e W h$. We generate the signal and background events by using MadGraph 5 and perform the parton shower and hadronization with PYTHIA [40]. The fast detector simulations are performed with Delphes [41], where the b-jet tagging efficiency and other basic cuts are taken as default value in delphes_card_ILD of ILC. FastJet [42] is used to cluster the jets by choosing the anti-k_t algorithm [43] with distance parameter $\Delta R = 0.4$.

Taking into account the current constraints, we take $m_T = 900, 1000, 1100$ GeV and $g^* = 0.3$ for three benchmark points. In order to suppress the backgrounds, we impose the following cuts

Table 1 Cut-flow cross sections of the signal and backgrounds at $\sqrt{s} = 2.0$ TeV with $g^* = 0.3$

Cuts	Signal(S)(fb)			Backgrounds(B)(fb)		
	$T900$	$T1000$	$T1100$	$\nu_e b \bar{t}$	$\nu_e W Z$	$\nu_e W h$
No cut	0.49	0.41	0.33	21.9	46.2	51.7
Cut-1	0.21	0.18	0.15	0.81	0.28	0.29
Cut-2	0.14	0.13	0.11	0.046	0.08	0.11
Cut-3	0.13	0.12	0.106	0.024	0.07	0.1
Cut-4	0.12	0.115	0.10	0.0237	0.057	0.09

Cut-1 : $\eta_l > -0.6$, $\Delta R(b_1, l) > 2.8$;

Cut-2 : $p_T(l) > 100$GeV, $p_T(b_1) > 160$GeV;

Cut-3 : $M_T(b_1 l) > 100$GeV;

Cut-4 : 65GeV $< M_{b_1 b_2} < 140$GeV.

where $M_T(b_1, l)$ is the transverse mass of the $b_1 l$ system and $M_{b_1 b_2}$ is the invariant mass of two b-jets.

We use MadAnalysis 5 [44,45] for analysis and summarize the cut-flow cross sections of the signal and backgrounds for the three benchmark points at $\sqrt{s} = 2.0$ TeV in Table 1. From the numerical results, we can see that the backgrounds are suppressed efficiently after imposing the selected cuts. The total cut efficiency of the signal can reach 24.5%, 28%, 30% for $m_T = 900, 1000, 1100$ GeV, respectively.

To estimate the observability quantitatively, we calculate the statistical significance (SS) by using Poisson formula [46]

$$SS = \sqrt{2L \left[(S + B) \ln \left(1 + \frac{S}{B} \right) - S \right]}, \quad (3)$$

where S and B are the signal and background cross sections and L is the integrated luminosity. Here, we have assumed the background uncertainty is negligible, which is the reason why it is possible to multiply by the luminosity L in front of the whole term in square brackets.

In order to investigate the top partner signal more comprehensively, we show the excluded regions depending on integrated luminosity at 2σ and 3σ level on the $g^* \sim m_T$ plane for $\sqrt{s} = 2.0$ TeV in (Fig. 4), where the conservative cut efficiency 25% of the signal is chosen. At 2σ level, we can see that the correlation region of $g^* \in [0.24, 0.5]$ and $m_T \in [800, 1360]$ GeV can be excluded with integrated luminosity $L = 100$ fb^{-1}. If the integrated luminosity can be raised to $L = 1000$ fb^{-1}, the excluded region will expand into $g^* \in [0.13, 0.5]$ and $m_T \in [800, 1620]$ GeV. If the 3σ evidence level is required, the higher integrated luminosity is needed to achieve the same excluded regions. Obviously, we can set the lower limits on the coupling parameter g^* according to the observed limits of the vector-like T mass and vice versa.
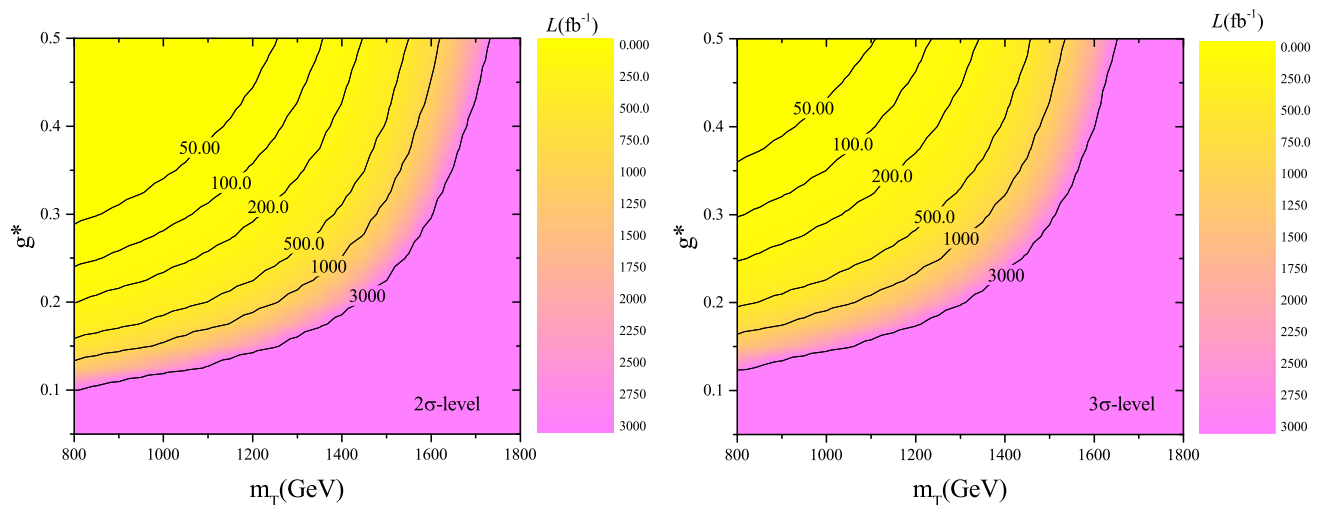
Fig. 4 Excluded regions depending on integrated luminosity at 2σ (left) and 3σ (right) level on the $g^* \sim m_T$ plane for $\sqrt{s} = 2.0$ TeV

4 Conclusions

In this paper, we study the single production of the vector-like top partner at the $e\gamma$ collision. In order to be as model-independent as possible, we exploited a simplified model, where the vector-like top partner is an $SU(2)$ singlet with charge 2/3. Under the current constraints, we caluclate the cross section and investigate the observability of the T through the channel $e^-\gamma \rightarrow \nu_e b\bar{T} \rightarrow \nu_e b W^-(\rightarrow l^-\bar{\nu}_l)\bar{b}$ at $\sqrt{s} = 2.0$ TeV. We find that the correlation region of $g^* \in [0.24, 0.5]$ and $m_T \in [800, 1360]$ GeV can be excluded corresponding to an integrated luminosity $L = 100\,\mathrm{fb}^{-1}$ at 2σ level. If the integrated luminosity can reach $L = 1000\,\mathrm{fb}^{-1}$, the excluded region will expand into $g^* \in [0.13, 0.5]$ and $m_T \in [800, 1620]$ GeV.

References

1. L. Susskind, Phys. Rev. D **20**, 2619 (1979)
2. J.A. Aguilar-Saavedra, R. Benbrik, S. Heinemeyer, M. Prez-Victoria, Phys. Rev. D **88**, 094010 (2013)
3. L. Panizzi, Nuovo Cim. C **037**, 69 (2014)
4. L. Randall, R. Sundrum, Phys. Rev. Lett. **83**, 3370 (1999)
5. H.-C. Cheng, B.A. Dobrescu, C.T. Hill, Nucl. Phys. B **589**, 249 (2000)
6. N. Arkani-Hamed, A.G. Cohen, E. Katz, A.E. Nelson, JHEP **07**, 034 (2002)
7. N. Arkani-Hamed, A.G. Cohen, E. Katz, A.E. Nelson, T. Gregoire, J.G. Wacker, JHEP **08**, 021 (2002)
8. M. Schmaltz, Nucl. Phys. Proc. Suppl. **117**, 40 (2003)
9. M. Schmaltz, D. Tucker-Smith, Ann. Rev. Nucl. Part. Sci. **55**, 229 (2005)
10. H.-C. Cheng, I. Low, L.-T. Wang, Phys. Rev. D **74**, 055001 (2006)
11. D. Marzocca, M. Serone, J. Shu, JHEP **08**, 013 (2012)
12. K. Agashe, R. Contino, A. Pomarol, Nucl. Phys. B **719**, 165 (2005)
13. ATLAS Collaboration, JHEP 10 (2017) 141, JHEP 08 (2017) 052
14. CMS Collaboration, CMS-B2G-17-003, CMS-B2G-17-007
15. G. Aarons et al., arXiv: 0709.1893; J. Brau et al., arXiv: 0712.1950;
16. H. Baer, T. Barklow, K. Fujii et al., arXiv:1306.6352
17. E. Accomando et al., hep-ph/0412251, CERN-2004-005; D. Dannheim, P. Lebrun, L. Linssen et al., arXiv:1208.1402;
18. H. Abramowicz et al., arXiv:1307.5288
19. I.F. Ginzburg, G.L. Kotkin, V.G. Serbo, Valery I. Telnov, Nucl. Instrum. Meth. **205**, 47–68 (1983)
20. JETP Lett. 34 (1981) 491-495; A. De Roeck, arXiv:hep-ph/0311138;
21. M. M. Velasco et al., eConf C010630 (2001) E3005;
22. V.I. Telnov, Nucl. Instrum. Meth. A **455**, 63 (2000)
23. B. Badelek et al., Int. J. Mod. Phys. A **19**, 5097 (2004)
24. M. Buchkremer, G. Cacciapaglia, A. Deandrea, L. Panizzi, Nucl. Phys. B **876**, 376 (2013)
25. S. Chatrchyan et al., CMS Collaboration. JHEP **1212**, 035 (2012)
26. F. del Aguila, M. Perez-Victoria, J. Santiago, JHEP **0009**, 011 (2000)
27. G. Cacciapaglia, A. Deandrea, L. Panizzi, N. Gaur, D. Harada, Y. Okada, JHEP **1203**, 070 (2012)
28. F.J. Botella, G.C. Branco, M. Nebot, JHEP **1212**, 040 (2012)
29. K. Ishiwata, Z. Ligeti, M.B. Wise, JHEP **1510**, 027 (2015)
30. A.K. Alok, S. Banerjee, D. Kumar, S.U. Sankar, D. London, Phys. Rev. D **92**, 013002 (2015)
31. F.J. Botella, G.C. Branco, M. Nebot, M.N. Rebelo, J.I. Silva-Marcos, Eur. Phys. J. C **77**, 408 (2017)
32. S.A.R. Ellis, R.M. Godbole, S. Gopalakrishna, J.D. Wells, JHEP **1409**, 130 (2014)

33. G. Cacciapaglia, A. Deandrea, N. Gaur, D. Harada, Y. Okada, L. Panizzi, JHEP **1509**, 012 (2015)
34. ATLAS Collaboration, ATLAS-CONF-2016-072
35. B.W. Lee, C. Quigg, H.B. Thacker, Phys. Rev. D **16**, 1519 (1977)
36. https://feynrules.irmp.ucl.ac.be/wiki/VLQ_tsingletvl
37. A. Alloul, N.D. Christensen, C. Degrande, C. Duhr, B. Fuks, Comput. Phys. Commun. **185**, 2250 (2014)
38. J. Alwall et al., JHEP **07**, 079 (2014)
39. C. Patrignani et al., Particle Data Group. Chin. Phys. C **40**(10), 100001 (2016)
40. T. Sjostrand, S. Mrenna, P.Z. Skands, JHEP **0605**, 026 (2006)
41. J. de Favereau et al., JHEP **1402**, 057 (2014)
42. M. Cacciari, G.P. Salam, G. Soyez, Eur. Phys. J. C **72**, 1896 (2012)
43. M. Cacciari, G.P. Salam, G. Soyez, JHEP **04**, 063 (2008)
44. E. Conte, B. Fuks, G. Serret, Comput. Phys. Commum. **184**, 222 (2013)
45. E. Conte, B. Dumont, B. Fuks, C. Wymant, Eur. Phys. J. C **74**, 3103 (2014)
46. G. Cowan, K. Cranmer, E. Gross, O. Vitells, Eur. Phys. J. C **71**, 1554 (2011)